British Journal of Cancer www.nature.com/bjc

ARTICLE

Molecular Diagnostics

IL-33/ST2 signaling promotes constitutive and inductive PD-L1 expression and immune escape in oral squamous cell carcinoma

Mengxiang Zhao[1,2,3,4], Yijia He[1,4], Nisha Zhu[1,4], Yuxian Song[1], Qingang Hu[1], Zhiyong Wang[2✉], Yanhong Ni[1✉] and Liang Ding[1✉]

BACKGROUND: Loss-of-function of PD-L1 induces therapy resistance of anti-PD-1/L1 therapy, and the complex regulatory mechanisms are not completely understood. We previously reported that stroma-derived interleukin-33 (IL-33) promoted the progression of oral squamous cell carcinoma (OSCC). We here focused on the immune-regulation role of IL-33 and its receptor ST2 signaling in PD-L1-positive OSCC patients.

METHODS: Activated T cells in in situ and peripheral blood were analyzed by IL-33/ST3 expression. Knockdown or overexpression of ST2 combined with IL-33/IFN-γ stimulation were performed to determine PD-L1 expression and PD-L1-dependent immune escape in OSCC/human T cells co-culture system, and OSCC orthotopic model based on humanized mouse with immune reconstitution and C57BL/6 mice models.

RESULTS: High IL-33/ST2 correlated with less activated T cells infiltration in situ and peripheral blood. Knockdown of ST2 down-regulated constitutive PD-L1 expression, whereas ST2 also promoted IL-33-induced PD-L1 Mechanistically, IL-33/ST2 activated JAK2/STAT3 pathway to directly promoted PD-L1 expression, and also activated MyD88/NF-κB signaling to up-regulate IFN-γ receptor (IFN-γR), which indirectly strengthen IFN-γ-induced PD-L1. Furthermore, ST2 is required for PD-L1-mediated immune tolerance in vitro and in vivo. $ST2^{high}$ OSCC patients have more PD-L1 and IFN-γR level in situ.

CONCLUSIONS: IL-33/ST2 signaling enhanced PD-L1-mediated immune escape, $ST2^{high}$ OSCC patients might benefit from anti-PD-1/L1 therapy.

British Journal of Cancer (2023) 128:833–843; https://doi.org/10.1038/s41416-022-02090-0

BACKGROUND

Antibodies directed against the programmed cell death-1 (PD-1) receptor have revolutionized the systemic therapy of advanced head and neck squamous cell carcinoma (HNSCC) [1, 2]. So far, the most commonly used predictor of therapeutic response to PD-1 blockade is the expression of PD-L1, a ligand of PD-1, on tumor cells [3]. However, a poor response rate to immune checkpoint blockade therapies in PD-L1-negative patients is a crucial problem to overcome [4, 5]. Therefore, it is critical to understand the molecular mechanism of tumor PD-L1 regulation, which is important for the improvement of anti-PD-L1/PD-1 therapy and its subsequent clinical effect. Currently, genetic events including PTEN deletions, EGFR mutations or JAK1/2 mutations etc. have been reported to preclude constitutive PD-L1 expression [6–8]. Moreover, stroma cells-derived, especially cytotoxic T cells, interferon-γ (IFN-γ) contribute to the inducible PD-L1 expression [9]. It is well-known that cytokines serve as mediators in shaping tumor microenvironment (TME) and facilitating tumor progression [10]. Previous studies have reported that CXCL12, IFN-γ and IL-6 promoted PD-L1 expression in cancer cells, but various mechanisms that regulate PD-L1 expression have already been described to be cell type-dependent [11–14].

Our team have been focusing on carcinoma-associated fibroblasts (CAF) in tumor growth and invasion, and immune regulation in oral squamous cell carcinoma (OSCC) [15–18]. Aberrant secretion of cytokines (TGF-β, IL-6, CCL22, IL-33, SDF-1 etc.) to tumor stroma is one of the features of CAFs. We reported that CAF-derived IL-33 promoted stromal fibroblast activation and proliferation of tumor cells in OSCC patients [15]. IL-33, a member of the IL-1 family, its role is to activate the immune system in response to tissue damage via interactions with its receptor ST2. Moreover, the IL-33/ST2 axis influences other elements of the TME, since it modifies the activity of T-helper lymphocytes via IL-4 and IL-13 [19]. Emerging evidences also show that IL-33/ST2 signaling

[1]Central Laboratory of Stomatology, Nanjing Stomatological Hospital, Medical School of Nanjing University, 22 Hankou Road, Nanjing 210093, China. [2]Department of Oral and Maxillofacial Surgery, Nanjing Stomatological Hospital, Medical School of Nanjing University, 30 Zhongyang Road, Nanjing 210008, China. [3]Department of Stomatology, Ningbo First Hospital, 59 Liuting street, Ningbo 315000, China. [4]These authors contributed equally: Mengxiang Zhao, Yijia He, Nisha Zhu. ✉email: wangzhiyong67@163.com; niyanhong12@163.com; 879269339@qq.com

Received: 22 June 2022 Revised: 17 November 2022 Accepted: 23 November 2022
Published online: 3 December 2022

play an important role in tumor progression, IL-33-directed ST2 signaling induced the preferential proliferation of tumor-infiltrating Tregs and enhanced tumor progression. Knockdown of IL-33/ST2 signaling decreased the accumulation of Tregs [20]. IL-33/ST2 signaling also induced immunosuppression of HNSCC by inducing IL-10 and TGF-β1 as well as decreasing the proliferation of responder T cells [21]. Accumulated evidences demonstrate that CAFs/tumor cells interaction is a critical regulator of immunosuppression via PD-1/L1 regulated T cell response [14]. However, the immune regulation role of IL-33/ST2 signaling in OSCC microenvironment remains to be unclear.

In this study, we analyzed the relationships between IL-33/ST2 signaling and PD-L1 expression in OSCC patients and cell lines, which was confirmed by knockdown or overexpression of ST2. The detail mechanisms of ST2/PD-L1 regulation were determined and the human peripheral blood mononuclear cells were isolated to establish $ST2^+$ OSCC/T cell co-culture system in vitro, humanized mouse models with no immunodeficiency and C57BL/6 mice in vivo to verify the ST2/PD-L1-mediated immune tolerance and tumor growth. Though these investigations, we test whether ST2 is potential predictors of PD-L1/PD-1 therapy efficacy for OSCC patients.

MATERIALS AND METHODS

Clinical sample collection and ethical approval

With the approval of the ethical committee of Nanjing Stomatology Hospital, Medical School of Nanjing University, oral tumors were collected from Nanjing Stomatology Hospital (No.2019NL-009(KS)). All the patients received radical surgery without any form of presurgical adjuvant therapy. Informed consent was provided by the patients for the use of their tissues and data. All animal experiments were performed in accordance with Jiangsu Association for Laboratory Animal Science (Authorization Number: 220195073) and were subject to review by the animal welfare and ethical review board of Nanjing university.

Immunohistochemistry (IHC) analysis

Sections of formalin-fixed and paraffin-embedded tissues were deparaffinized and subjected to antigen retrieval using 10 mM citrate buffer (92 °C for 30 min). Gene expression was evaluated according to stain intensity and the percentage of positive cells. The intensity of staining was graded as 1 = weak staining, 2 = moderate staining and 3 = strong staining. The percentage of stained cells was graded as 0 = 0–5%, 1 = 6–25%, 2 = 26–50%, 3 = 51–75% and 4 = 75–100%. The final score was obtained by multiplying the two scores. All scorings were conducted by two pathologists without knowledge of the patients' clinical characteristics or outcome.

Isolation and primary culture of fibroblasts

OSCC specimens and adjacent normal tissues were harvested within 30 min after surgical resection. Harvested tissues were placed in DMEM/F-12 supplemented with 10% FBS and antibiotics (Invitrogen Corporation) for immediate transportation on ice to the laboratory. NFs and CAFs isolated from tissues by combining mechanical and enzymatic methods. Tissues were performed in detail as previously described [15]. The sterile fresh OSCC tissues and its corresponding normal tissues were washed with PBS and antibiotics, and eliminated the epithelial and adipose tissues. The specimens were sliced into small pieces and digested by enzyme mixture (Collagenase, Neutral protease, Hyaluronidase) for 30 min. The remaining small tissues incubated in DMEM/F12 medium with 20% fetal bovine serum at 37 °C. The medium was replaced every 2–3 days and the epithelial cells were removed via trypsinization, the remaining cells were fibroblasts.

Cell culture

HN6, Cal27, Hsc3 and SCC7 cells were maintained in Dulbecco's Modified Eagle's Medium (Invitrogen), supplemented with 10% fetal bovine serum (FBS) and 1% penicillin–streptomycin.

Reagents

p-STAT3(#9145), p-JAK2(#3771), PD-L1(#13684), JAK2(#3230), STAT3(#9139), NF-κB (#8242), p-NF-κB (#3033) were obtained from Cell Signaling Technology. ST2 (#ab25877), IL-33 (#ab54385), IFNGR1 (#ab134070), CD8 (#ab237710/ab217344) and Foxp3 (#ab215206) were obtained from the Abcam company. Secondary anti-rabbit IgG Dylight 680 (#35568), anti-rabbit IgG Dylight 488 (#35553) and anti-mouse IgG Dylight 800 (#35521) were obtained from ThermoFisher. Recombinant human IL-33 protein (3625-IL) was obtained from R&D Systems. Recombinant Mouse IL-33 Protein (3626-ML) was obtained from R&D Systems.

RNA analysis

RNA was obtained using Trizol reagent following the manufacturer's procedure and then reversed into cDNA using HiScript III RT SuperMix (Vazyme Biotech Co., Ltd). The relevant expression of the genes was determined via AceQ® qPCR SYBR® Green Master Mix (Vazyme Biotech Co., Ltd). Transcriptome sequencing of three cell lines was performed by Shanghai OE Biotech. Co., Ltd.

T cell-mediated tumor cell killing assay

PBMC were cultured in CTS™ AIIM V™ SFM (A3021002; Gibco) with ImmunoCult Human CD3/CD28/CD2 T cell activator (10970; STEMCELL Technologies) and Recombinant Human IL-2 (1000 U/mL, 202-1L-050, R&D) for one week according to the manufacturer's protocol. The experiments were performed with anti-CD3 antibody (100 ng/mL; 16-0037; eBioscience, Thermo Scientific), IL-2 (1000 U/mL). Cancer cells were allowed to adhere to the plates overnight and then incubated for 48 h with activated T cells. Different proportion between cancer cells and activated cells (1:3) were utilized according to the purpose of each experiment. T cells and cell debris were removed by PBS wash, and living cancer cells were then quantified by a spectrometer at OD (570 nm) followed by crystal violet staining.

Lentivirus vectors

The GFP-labeled Lentivirus-mediated overexpression vector containing IL1RL1(Lv- IL1RL1) was used to stably overexpressing ST2 in OSCC cells, with Lv-ctrl as the matched controls (GENECHEM, Shanghai, China and OBiO Technology Co. Ltd., Shanghai, China) according to the manufacturer's instruction. The GFP-labeled Lentivirus vector expressing sh-IL1RL1 (Lv-shIL1RL1) was used to stably knock down ST2 expression (GENECHEM, Shanghai, China and OBiO Technology Co. Ltd., Shanghai, China). The cells were treated with puromycin (5 μg/mL) for 2 weeks to establish stable cell lines.

Cell transfection

Cells were grown on 6/12 wells plate to 60% confluence and transfected the plasmid of overexpression or knockdown of ST2 using Lipofectamine 2000 (Invitrogen) according to the manufacturer's instructions and a final concentration was 60 nM. At 48 h after transfection, cells were harvested for qPCR or Western blot analysis. Similarly, transient transfection of siRNAs targeting the *MYD88* and *TRAF6* (50 nM) into HN6 cells was performed in the presence of lipofectamine RNAiMAX (Invitrogen) for 24 h according to the manufacturer's instructions, and cells were harvested for qPCR analysis.

Immunofluorescence

Cells were seeded on coverslips in 24-well plate and cultured overnight. Subsequently cells were fixed in 4% paraformaldehyde, permeabilized in 0.2% Triton X-100 at room temperature, and then incubated with primary antibody overnight at 4°C after 5%BSA blocking for 1 h. After incubating 2 h at room temperature with secondary antibody, the coverslips were counterstained with 0.2 mg/ml DAPI and followed by washing PBS. Sealed with nail polish and observed under FV3000 confocal microscope (OLYMPUS, Japan). Tissues immunofluorescence was performed as the description of cells immunofluorescence.

Western blot analysis

Cells were lysed in buffer containing 50 mmol/L Tris–HCl, pH8.0, 150 mmol/LNaCl, 0.02% NaN3, 0.1 %SDS, 100 mg/L phenylmethylsulfonylfluoride, 1 mg/L aprotinin, and 1% Triton. Cell extract was separated by SDS-PAGE and transferred onto PVDF membranes. The membranes were blocked for 1 h in TBST (10 mmol/L Tris–HCl, pH 7.4,150 mmol/L NaCl, 0.05% Tween-20) containing 5% bovine serum albumin (BSA), incubated with primary antibodies at 4 °C overnight and then incubated with secondary antibodies. Bands were visualized with enhanced chemiluminescence reaction (Millipore Corp.). GAPDH was used as the loading control. Protein bands were captured and analyzed using the Lane 1D software (Sage Creation Science Co, Beijing).

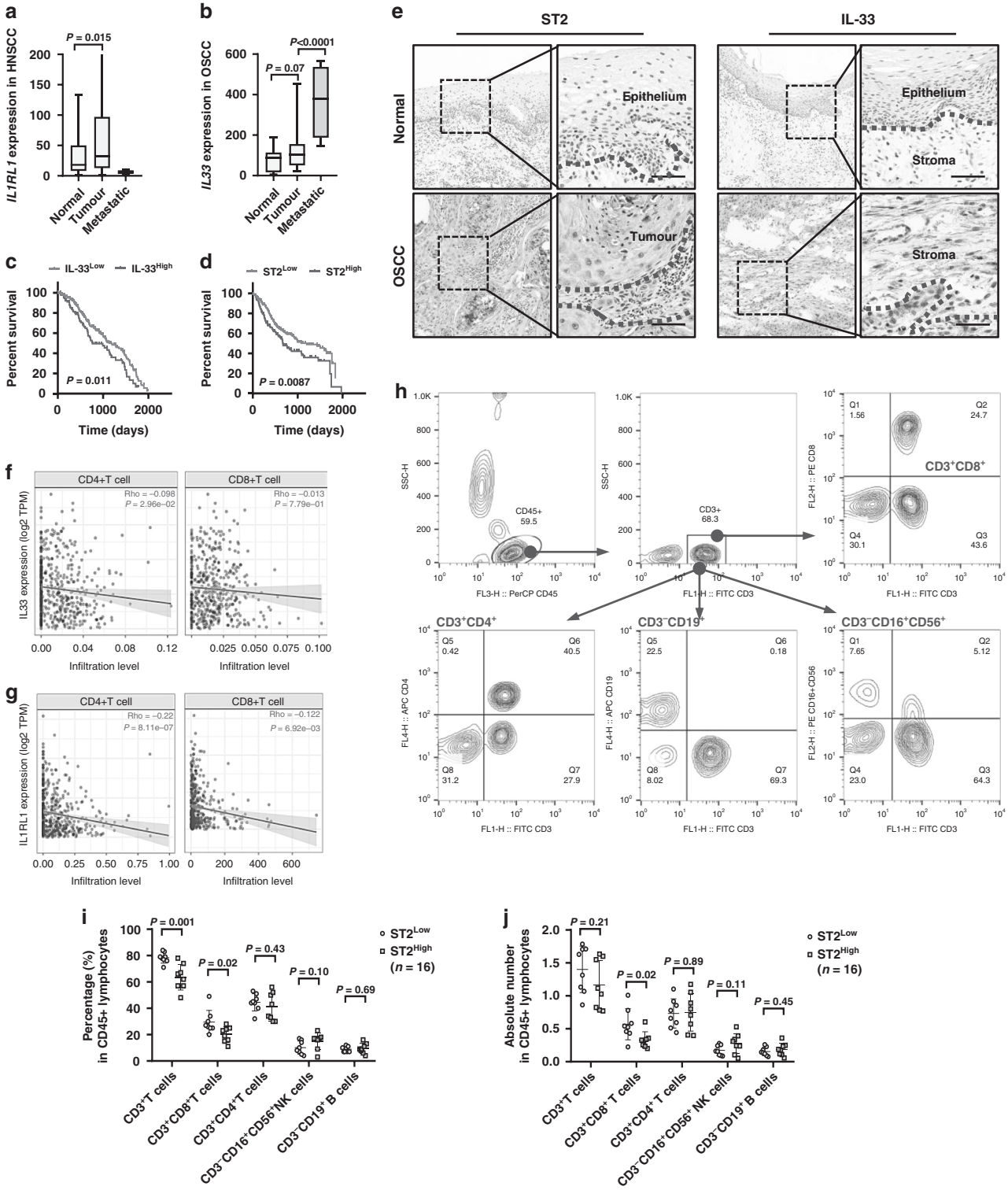

Fig. 1 Correlations between IL-33/ST2 and T cells activation in situ and blood. a, **b** Expressions of ST2 in HNSCC and IL-33 in OSCC were analyzed by database (https://tnmplot.com/analysis/). **c**, **d** The effect of ST2 and IL-33 expression on the prognosis of OS in HNSCC patients were showed by Log-rank (Mantel-Cox) test. **e** IHC results of expression pattern of ST2 and IL-33 in OSCC ($n = 6$). **f**, **g** Correlation between ST2/IL-33 expression and $CD4^+$T cell, $CD8^+$T cell infiltration in HNSCC from TIMER2.0 database. **h** The ratio and absolute number of human $CD3^+$ T cells, $CD3^+CD4^+$ helper/inducer T cells, $CD3^+CD8^+$ cytotoxic T cells, $CD3^-CD19^+$ B cells, and $CD3^-CD16^+$ and/or $CD56^+$ NK cells in blood were analyzed in ST^{Low} and ST^{High} groups by BD Multitest™ reagent in the blood of OSCC patients ($n = 16$). Results are shown as mean ± SEM. $^*p < 0.05$, $^{**}p < 0.01$, $^{***}p < 0.001$. p = two-tailed t test.

Experimental animals

Female NOD/ShiLtJGpt-*Prkdc*^{em26Cd52}*Il2rg*^{em26Cd22}/Gpt (NCG) mice and C57BL/6 mice were obtained from Gempharmatech Co., Ltd (China) and were used between 6 and 8 weeks of age. The mice were maintained under pathogen-free conditions according to SPF guideline (room temperature, 40–60% humidity).

Preparation of PBMC

Fresh whole blood from patients was collected with EDTA tube (ethylenediamine tetraacetic acid tube, BD Vacutainer). On average, 1.0×10^7 cells were isolated from 5 ml of whole blood. The collected whole blood was 2× diluted with Hanks' Balanced Salt solution (HBSS, Gibco, Rockville, MD, USA) for loading on Ficoll-paque (Pharmacia, Uppsala, Sweden). The blood-loaded sample on Ficoll solution is centrifuged at 2000 rpm for 20 min (Acceleration /Break = lowest /zero), and middle layer was collected as PBMC. The collected cells were enumerated and stored in liquid nitrogen tank until us. All study participants provided informed consent, and was approved by the ethical committee of Nanjing Stomatology Hospital, Medical School of Nanjing University.

PBMC injection process for Hu-PBL-NCG mouse tumor model

The PBMC from healthy patients was stored in liquid nitrogen tank until use. The restored PBMC is washed one time with HBSS (Gibco), and finally mixed with 200 µl of HBSS (Gibco) for intravenous injection in the tail of recipient mouse (NCG mouse). Injection of $1–2 \times 10^7$ PBMCs in the lateral side of tail vein was performed.

To generate an orthotopic xenograft tongue tumor model, conditional 2.5×10^5 HN6 OSCC cells were suspended in 20 µL of PBS/Matrigel (3:1) and injected into the anterior portion of the tongue of Hu-PBL-NCG mouse using a syringe with a 30 gauge needle (BD Biosciences). On day 7-10 after injection, mice were randomly divided into different treatment groups.

In orthotopic xenograft tongue tumor model of C57BL/6 mice with no immunodeficiency, control or ST2-knockdown SCC7 cells were used. Anti-mPD-L1 (clone 10 F.9G2, catalog no. BP0101–2, BioXcell) or IgG isotype control (catalog no. BP0090, BioXcell) was treated, 200 µg/mice, i.p., every 2 days. Tumor weight were determined, and $CD8^+$ T cells, $Foxp3^+$ Tregs in tumor tissues were analyzed by immunohistochemistry. All tumors were measured using calipers by technicians blinded to the aims of the study and the hypothesized outcome.

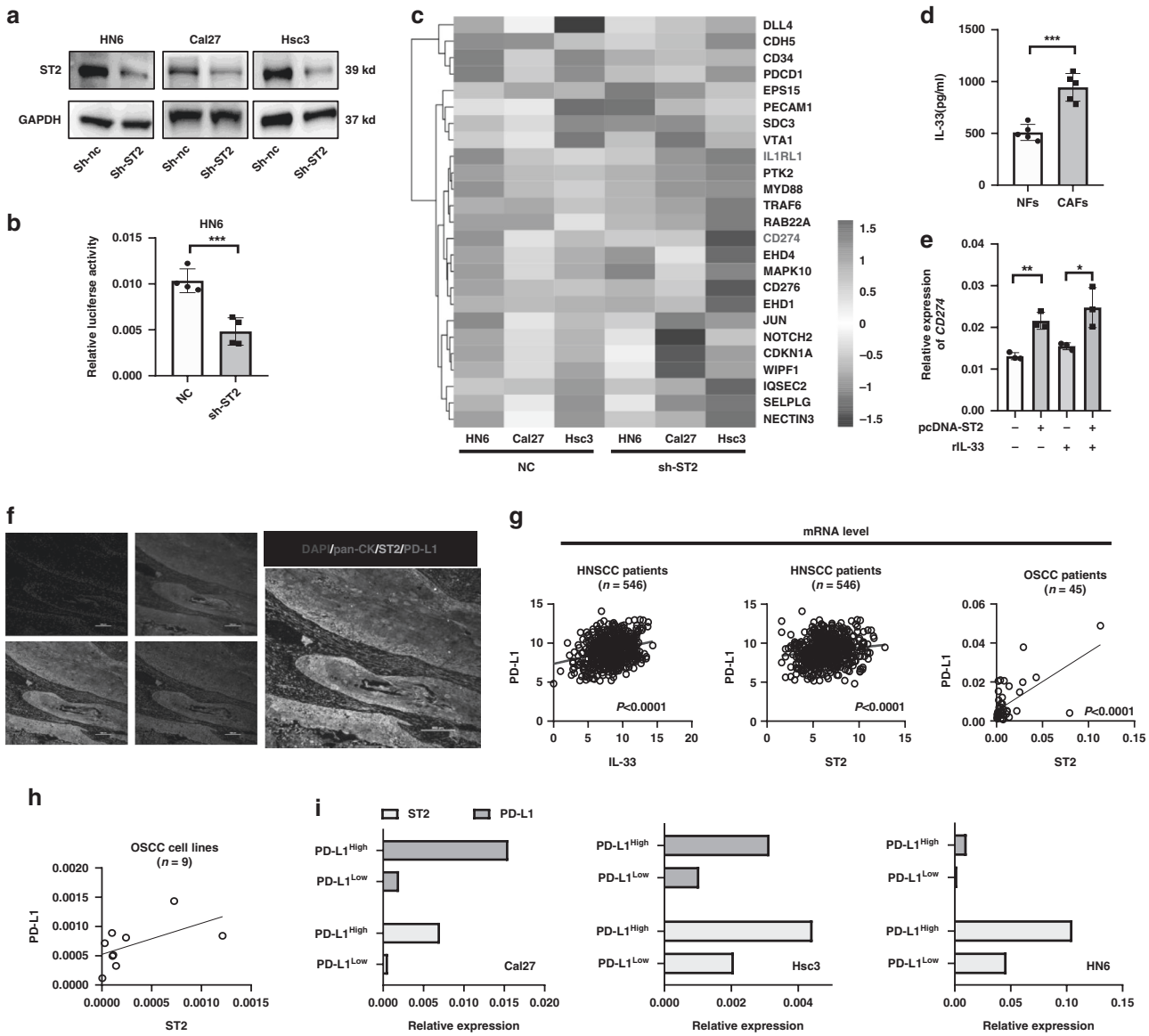

Fig. 2 IL-33/ST2 signal in OSCC regulates the expression of PD-L1. a Knockdown effect of ST2 in HN6, Cal27 and Hsc3 by WB analysis. **b** Luciferase activity in CD274 promoter region after ST2 knockdown. **c** Transcriptome sequencing of ST2 knockdown cell lines. **d** ELISA showed an increased IL-33 level in medium from CAFs compared with NFs. **e** Overexpression of ST2 promoted IL-33-induced PD-L1 expression. **f** The expression and localization of PD-L1 and ST2 were analyzed by immunofluorescence staining. **g** The mRNA expression correlation between IL-33/ST2 and PD-L1 was analyzed by database (http://www.cbioportal.org/) and in 45 cases of oral squamous cell carcinoma. **h** The expression of ST2 and PD-L1 in 9 oral cancer cell lines detected by qPCR. **i** Expression of ST2 in PD-L1^{high} and PD-L1^{Low} sorting cell line detected by qPCR. Results are shown as mean ± SEM. *$p < 0.05$, **$p < 0.01$, ***$p < 0.001$. p = two-tailed t test.

Statistics

Statistical analysis was performed using GraphPad Prism (San Diego, CA). Two-tailed Student's *t* tests were used for comparison of experimental groups. Statistical significance was defined at equal to or more than 95% confidence interval or $P < 0.05$. The experiments presented are representative of 3 different repetitions. Data are presented as Mean ± standard deviation.

RESULTS

High IL-33/ST2 level in OSCC tissues is associated with less $CD8^+$ T cell infiltration in situ and in blood

We firstly analyzed the expression of IL-33 and ST2 in tumor tissues and normal tissues in HNSCC and OSCC by database (https://tnmplot.com/analysis/). In HNSCC patients, the expression of ST2 in tumor tissues was significantly higher than that in normal tissues (Fig. 1a). IL-33 was also up-regulated in tumor tissues of OSCC and further enriched in metastatic niche (Fig. 1b). Consistently, our previous study demonstrated that OSCC patients with advanced TNM stage and tumor proliferation showed high-expressed IL-33. The prognostic value of IL-33 and ST2 in HNSCC patients were determined and found that patients with high ST2 had short overall survival time (Fig. 1d) and patients with high IL-33 had worse OS than those with low IL-33 expression (Fig. 1e). We also determined the expression patterns of IL-33 and ST2 in 30 OSCC tissues were evaluated by immunohistochemical (IHC) staining. The results showed that the expressions of ST2 and IL-33 were absent in normal epithelium and up-regulated during carcinogenesis. In OSCC, ST2 was mainly expressed in tumor cells, while IL-33 showed more stromal expression in CAFs and vascular endothelial cells, which was consistent with our previous study [15] (Fig. 1c).

Moreover, we evaluated the correlation between the expression of IL-33/ST2 and $CD4^+$ or $CD8^+$ T cells in HNSCC patients based on TCGA database. The results showed that there was a significant negative correlation between the expression of ST2/IL-33 and the infiltration of $CD4^+$ T cells (Fig. 1f, h) and $CD8^+$ T cells (Fig. 1g, i) in the tumor microenvironment. Furthermore, using our biobank and clinical laboratory as previously reported [16, 22], we retrospectively analyzed the ratio and absolute number of key immunocytes in the blood of OSCC patients ($n = 16$) according to ST2 expression. Human $CD3^+$ T cells, $CD3^+CD4^+$ helper/inducer T cells, $CD3^+CD8^+$ cytotoxic T cells, $CD3^-CD19^+$ B cells, and $CD3^-CD16^+$ and/or $CD56^+$ NK cells were analyzed in $ST2^{high}$ and $ST2^{low}$ groups. Results showed that

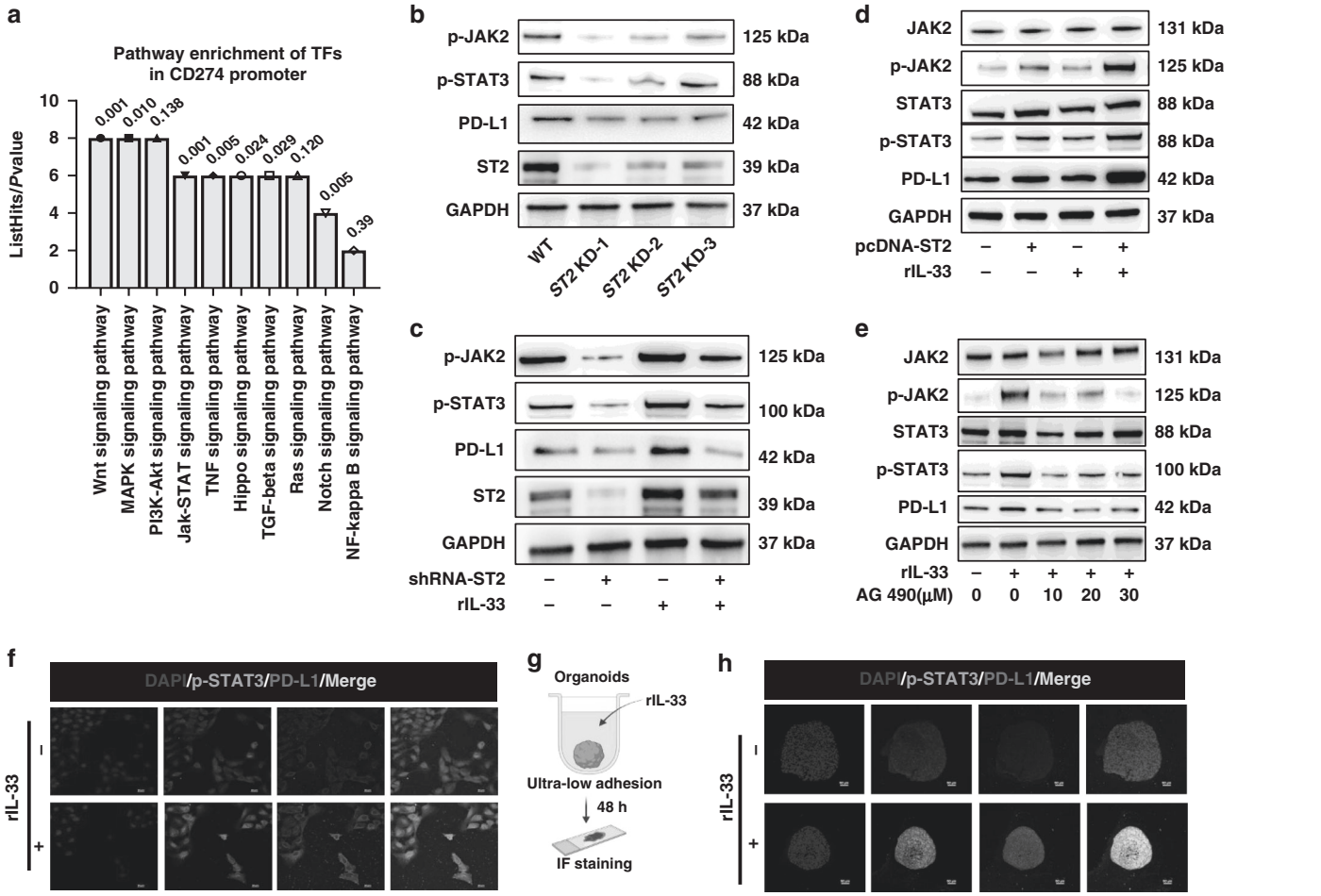

Fig. 3 The role of JAK2/STAT3 pathway in the regulation of PD-L1 expression by IL-33/ST2. a Pathway enrichment analysis of potential TFs in PD-L1 promoter region. **b** Western blot showed PD-L1 expression and JAK2/STAT3 phosphorylation in tumor cells after ST2 knockdown. **c** The protein level of JAK2/STAT3 activation and PD-L1 expression in tumor cells stimulated by IL-33 after knockdown of ST2 (25 ng/ml). **d** Western blot was used to analyze the activation of JAK2/STAT3 pathway and the expression of PD-L1 in tumor cells stimulated by IL-33 after overexpression of ST2. **e** Western blot was used to analyze the effect of AG490 on the phosphorylation of JAK2/STAT3 pathway and the expression of PD-L1 under different concentrations of IL-33 stimulation. **f** The effect of IL-33 stimulation on the expression of PD-L1 and p-STAT3 in HN6 cells was analyzed by cellular immunofluorescence. **g**, **h** Immunofluorescence analysis of the effect of IL-33 stimulation on the expression of PD-L1 and p-STAT3 in 3D tumor spheres of HN6. Results are shown as mean ± SEM. *$p < 0.05$, **$p < 0.01$, ***$p < 0.001$. p = two-tailed *t* test.

patients with high ST2 had relatively low ratio and numbers of $CD3^{+}CD8^{+}$ cytotoxic T cells in blood.

IL-33/ST2 signaling promote PD-L1 expressions in oral squamous cell carcinoma cells

To uncover the potential connection between ST2 and decreased activated T cells, we obtained three cell lines to acquire stable knockdown of ST2 by transfecting Cal27, HN6 and Hsc3 OSCC cell lines via lentivirus-shRNA-ST2. The knockdown efficiency was verified by WB (Fig. 2a). We constructed the luciferase plasmid containing the promoter region of PD-L1, and found that luciferase activity decreased significantly in ST2 knockdown tumor cells (Fig. 2b). Transcriptome sequencing of three cell lines indicated that *CD274* (encod PD-L1) were

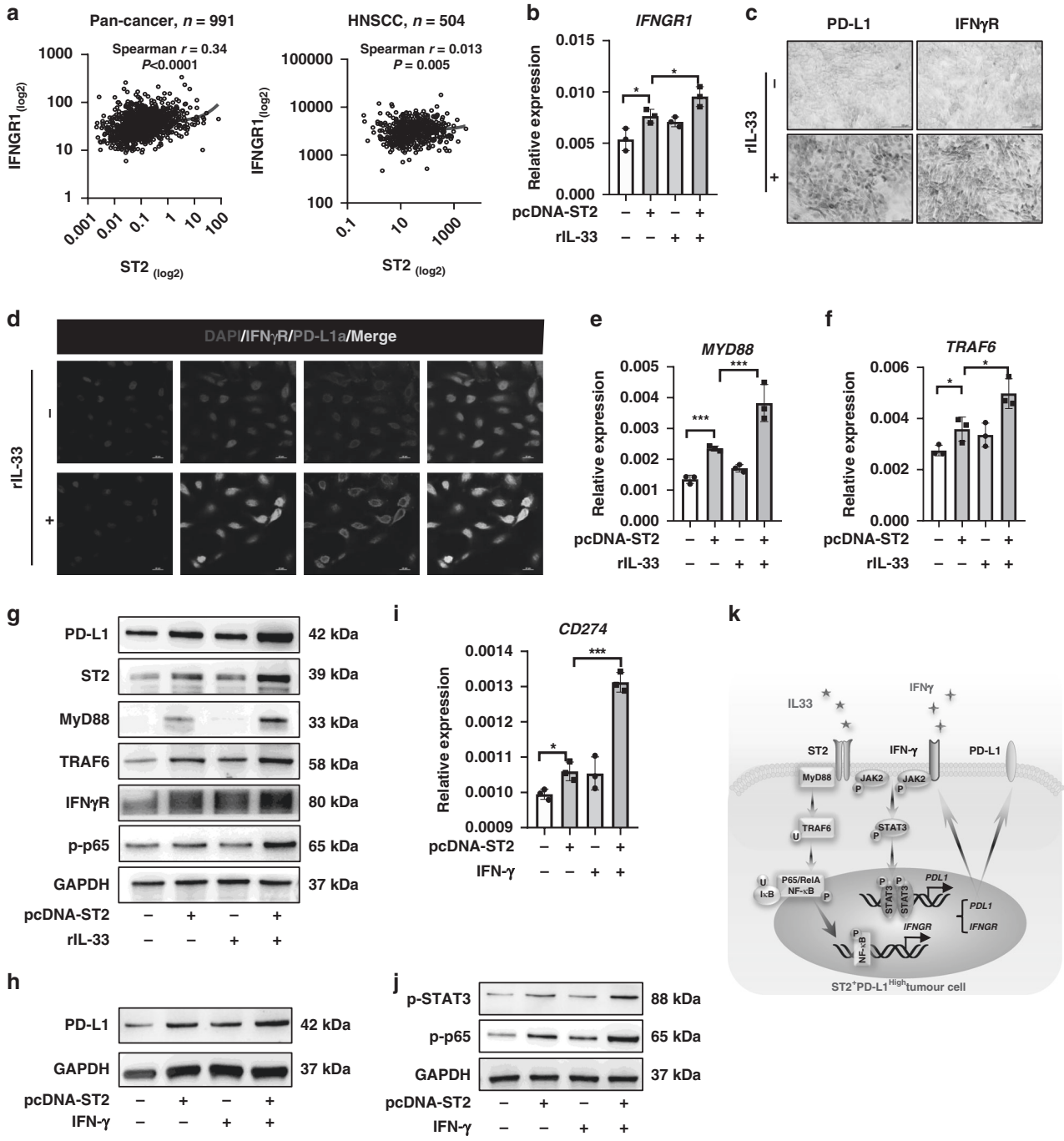

Fig. 4 The impacts of IL-33/ST2 signaling on IFN-γR/PD-L1 expression of tumor cells. a The mRNA expression correlations between *IFNGR* and *ST2* in pan-cancer and HNSCC were analyzed by database (http://www.cbioportal.org/). Immunocytochemical analysis showed that IL-33 stimulates PD-L1 and IFN-γR expression in HN6 cells. **b** *IFNGR* mRNA expression level in $ST2^{OE}$ HN6 cells under IL-33 stimulation. **c**, **d** Immunofluorescence and immunocytochemistry of IFN-γR and PD-L1 by IL-33 stimulation. **e**, **f** qPCR analysis showed the mRNA expression of MYD88 and TRAF6 when IL-33/ST2 signal was activated. **g** The protein levels of IFN-γR, PD-L1 and MyD88/TRAF6/NF-κB pathway were determined by WB. **h**, **i** PD-L1 mRNA and protein expression level in $ST2^{OE}$ HN6 cells under IFN-γ stimulation. **j** Western blot of NF-κB and STAT3 phosphorylation in HN6 cells in response to ST2 signaling and IFN-γ stimulation. **k** The model of ST2 signaling-regulated PD-L1 expression in OSCC. Results are shown as mean ± SEM. $^{*}p < 0.05$, $^{**}p < 0.01$, $^{***}p < 0.001$. p = Two-tailed t test.

significantly reduced in ST2 knockdown cell lines (Fig. 2c). Correspondingly, MyD88/TRAF6, as ST2 downstream adapter protein, were also inhibited by ST2 knockdown. ELISA results confirmed our previous finding that the secretion of IL-33 in CAFs was significantly higher than that in NFs (Fig. 2d). After stimulated by recombinant human IL-33 cytokine (25 ng/ml), ST2 overexpressed ($ST2^{OE}$) HN6 cell line showed significant up-regulated *CD274* expression, indicating that ST2 activation is required for PD-L1 expression (Fig. 2e).

In order to clarify the co-expression in situ of ST2 and PD-L1 in OSCC tissue, we performed immunofluorescence staining on 10 frozen OSCC tissue sections, pan- keratin^{+} tumor cells simultaneously showed ST2 and PD-L1 positive staining and co-localization (Fig. 2f). Similarly, through the correlation analysis of

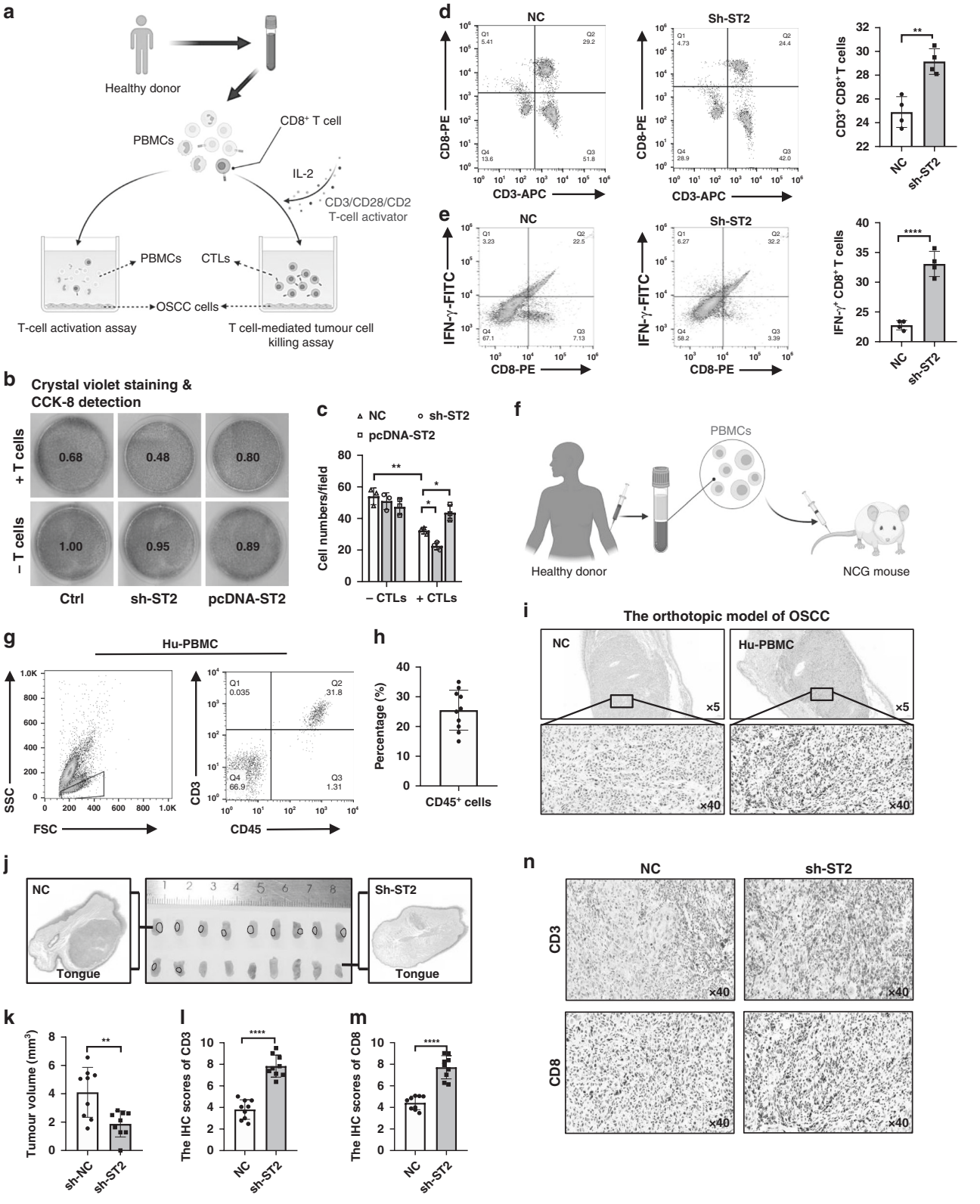

Fig. 5 ST2 knockdown promote the human CTL killing function in vitro and in vivo of Hu-PBMC mouse model. a Schematic diagram of T cell-mediated tumor cell killing assay and T cell activation assay. **b** T cell-mediated cancer cell-killing assay results. HN6 cells cocultured with activated T cell for 48 h were subjected to Crystal violet staining and CCK-8 detection. **c** Numbers of live tumor cells were counted. **d**, **e** After co-cultured with ST2 knockdown HN6, the percentage of $CD3^+$ $CD8^+$ T cells and $CD8^+IFN\text{-}\gamma^+$ T cells in PBMC were analyzed. **f** Schematic diagram of Hu-PBMC mouse model construction. **g**, **h** After 10 days of PBMC transplantation ($1–2*10^7$ per mice, i.v.), the $CD45^+CD3^+$ T cell integration rate was tested in tail blood sampling. **i** The infiltration of $CD8^+$ T cells in orthotopic OSCC model in Hu-PBMC mouse. **J**, **k** Transplanted tumor in mice tongue and representative diagram of HE staining. **l**, **n** The infiltration of $CD3^+$T and $CD8^+$T cells in ST2 knockdown group and control group was analyzed by immunohistochemistry. Results are shown as mean ± SEM. $*p < 0.05$, $**p < 0.01$, $***p < 0.001$. p = Two-tailed t test.

IL-33, ST2 and PD-L1 in HNSCC patients by database (http://www.cbioportal.org/), we found that IL-33 and ST2 (Fig. 2g) had a significant positive correlation with the expression of PD-L1, respectively. We also collected RNA samples from 45 OSCC tissues and confirmed that $ST2^{high}$ patients also have higher PD-L1 level (Fig. 2h). Similar findings were found in 9 OSCC cell lines (including Cal27, Cal33, Scc4, Scc9, Scc131, Scc172, Hsc2, Hsc3 and HN6) (Fig. 3h). In turn, we sorted PD-$L1^{low}$ and PD-$L1^{high}$ cells in three OSCC cell lines by Flow cytometry (Cal27, Scc9 and Hsc3). qPCR analysis showed that the expression of ST2 in PD-$L1^{low}$ cells was significantly lower than that in PD-$L1^{high}$ cells (Fig. 2i).

IL-33/ST2 signaling promote constitutive PD-L1 expression via JAK/STAT3 pathway

In order to identify the key pathway orchestrating the PD-L1 expression in $ST2^{high}$ tumors, we performed a Genome Transcription Regulation Database (GTRD) database analysis (http://gtrd.biouml.org/). Several predicted transcriptional factors (TFs) binding sites in the *CD274* promoters were found. Through KEGG enrichment analysis of these TFs, the JAK/STAT pathway significantly harbor the TFs targeting the *CD274* promoters, which was consistent with previous findings [3, 7] (Fig. 3a). Thus we detected the activation of JAK2 and STAT3 in OSCC cell with ST2 knockdown. Results found that the phosphorylation of JAK2 and STAT3 both reduced by ST2 inhibition (Fig. 3b). Moreover, although the stimulation of IL-33 cytokine could significantly up regulate the phosphorylation degree of JAK2 and STAT3, ST2 knockdown could suppress JAK2/STAT3 pathway activation (Fig. 3c). In contrast, the phosphorylation of JAK2/STAT3 was enhanced in $ST2^{OE}$ OSCC cell lines (Fig. 3d). To confirm the role of JAK/STAT pathway in PD-L1 transcription, JAK2 inhibitor AG490 was treated. Results showed that the phosphorylation of JAK2 and STAT3 gradually decrease by AG490, accompanied by the down-regulation of PD-L1 expression (Fig. 3e).

The immunofluorescence results also showed that the expression of PD-L1 and the nucleus staining of p-STAT3 were enhanced by IL-33 stimulation (25 ng/ml) (Fig. 3f). To investigate the IL-33/ST2/PD-L1 pathway further, we co-cultured the HN6 OSCC cell line with IL-33 in an ultra-low adhesive environment to form 3D tumor organoid (Fig. 3g). The immunofluorescence staining results confirmed that IL-33/ST2 activation could activate p-STAT3 nuclear localization and increase PD-L1 expression. (Fig. 3h).

IL-33/ST2 signaling up-regulates IFN-γR expression via MyD88 to enchance IFN-γ-mediated inductive PD-L1 expression

Clinical data from pan-cancer and HNSCC patients cohorts showed that *CD274* was positively correlated with *IFNGR* (http://www.cbioportal.org/) (Fig. 4a). RNA-sequence indicated that *IFNGR* was down-regulated by ST2 knockdown in OSCC cell lines (Fig. 2c), whereas IFN-γ/IFN-γR activation is critical event for PD-L1 induction during targeting therapy [9, 23], thus we speculate that IL-33/ST2 signal may indirectly enhances IFN-γ/PD-L1 pathway activation by IFN-γR. Indeed, overexpression of ST2 enhanced IL-33-induced *IFNGR* up-regulation (Fig. 4b). The effect of IL-33/ST2 activation on IFN-γR level was confirmed by immunocytochemistry and immunofluorescence staining (Fig. 4c, d).

MyD88 and TRAF6, as the downstream signal molecules of ST2 [24, 25], is reported to induce NF-κb activation which is necessary for *IFNGR* transcription [26, 27]. IL-33/ST3 activation promoted *MYD88* and *TRAF6* expression (Fig. 4e–f), which was verified by WB analysis (Fig. 4g). At the same time, the phosphorylation of NF-κB and IFN-γR were also up-regulated under the stimulation of IL-33/ST2 signal (Fig. 4g). *MYD88* and *TRAF6* was knocked down by siRNA in $ST2^{High}$ HN6 cells and was found to impair *IFNGR* expression. Moreover, in response to IFN-γ treatment, IL-33/ST2 activation require MyD88 and TRAF6 to regulate IFN-γ/IFN-γR/PD-L1 pathway, which could be inhibited by MyD88 knockdown (Supplementary Fig. 1a–c). Combination of ST2 overexpression and IFN-γ stimulation induced a further increase in the gene and protein level of PD-L1 was observed (Fig. 5h, i), which was involved with activated STAT3 and p65 (Fig. 5j). Therefore, these data indicated that ST2 signaling could directly promote PD-L1 expression via JAK-STAT3 pathway, and indirectly promote IFN-γR expression to further enhance IFN-γ-mediated PD-L1 induction (Fig. 5k).

$ST2^{High}$ tumor cells inhibit the tumor killing function of human $CD8^+$T cells through PD-L1

To estimate the role of $ST2^+$ tumor cells in immune escape, we established tumor/immunocytes co-culture system. We sorted $CD8^+$ T cells in human peripheral blood mononuclear cells (PBMCs) by magnetic bead, CD3/CD28 activator and IL-2 cytokine were used to stimulate the expansion of $CD8^+$ T cells and induce the activation of cytotoxic T lymphocyte (CTLs) (Fig. 5a). T cell-mediated tumor cell-killing assays showed that activated $CD8^+$ T cells efficiently promoted $ST2^+$ tumor death, which was further strengthened by ST2 knockdown. Overexpression of ST2 in HN6 cells, in turn, rendered the cells more resistant to human CTLs (Fig. 5b, c). Meanwhile, T cell activation ratio in the supernatant was detected by flow cytometry. The results showed that compared with the control group, the proportion of $CD3^+CD8^+$ T cells and $CD8^+IFN\text{-}\gamma^+$ T cell in $CD3^+$ T cells was significantly up-regulated in HN6 group with ST2 knockdown (Fig. 5d, e).

To provide more evidence in vivo, we transplanted NCG mice ($NOD^{prkdc\text{-}/\text{-}il\text{-}2rg\text{-}/\text{-}}$) mice with human peripheral blood mononuclear cells (PBMCs) (i.p. $2*10^7$ /mice) for immune reconstitution to establish a new humanized PBMC (hu-PBMC) mouse model. (Fig. 6f). After 10 days of PBMC injection, the efficiency of reconstitution was analyzed by flow cytometry and results showed that the average ratio of $CD45^+$ cells was ~20-30% and the human $CD45^+CD3^+$ T cells in the peripheral blood of mice were clustered (~80%) (Fig. 5g, h). We further established an orthotopic model of OSCC in NCG mice and Hu-PBMC mice by injecting human OSCC cell line HN6 into the tongue, and found that the infiltration of $CD8^+$ T cells in tumor were only detected in Hu-PBMC group (Fig. 5i). $ST2^{KD}$ HN6 cells were used for tongue tumor implantation and the tumor volume in $ST2^{KD}$ group was significantly smaller than that in control group (Fig. 5j, k). Immunohistochemical staining was performed to detect the infiltration of $CD3^+$ T cells and $CD8^+$ T cells in the tumor (Fig. 5l, n). The staining results showed that the infiltration of $CD3^+$ T cells and $CD8^+$ T cells in the transplanted tumor of $ST2^{KD}$ group was higher than that in the control group.

ST2 knockdown combines with anti-PD-L1 therapy show superior anti-tumor effects in OSCC

We assessed the immunosuppressive effect of IL-33/ST2 signals on $CD8^+$ T cells in the presence of anti-PD-(L)1 blocking Ab. C57BL/6

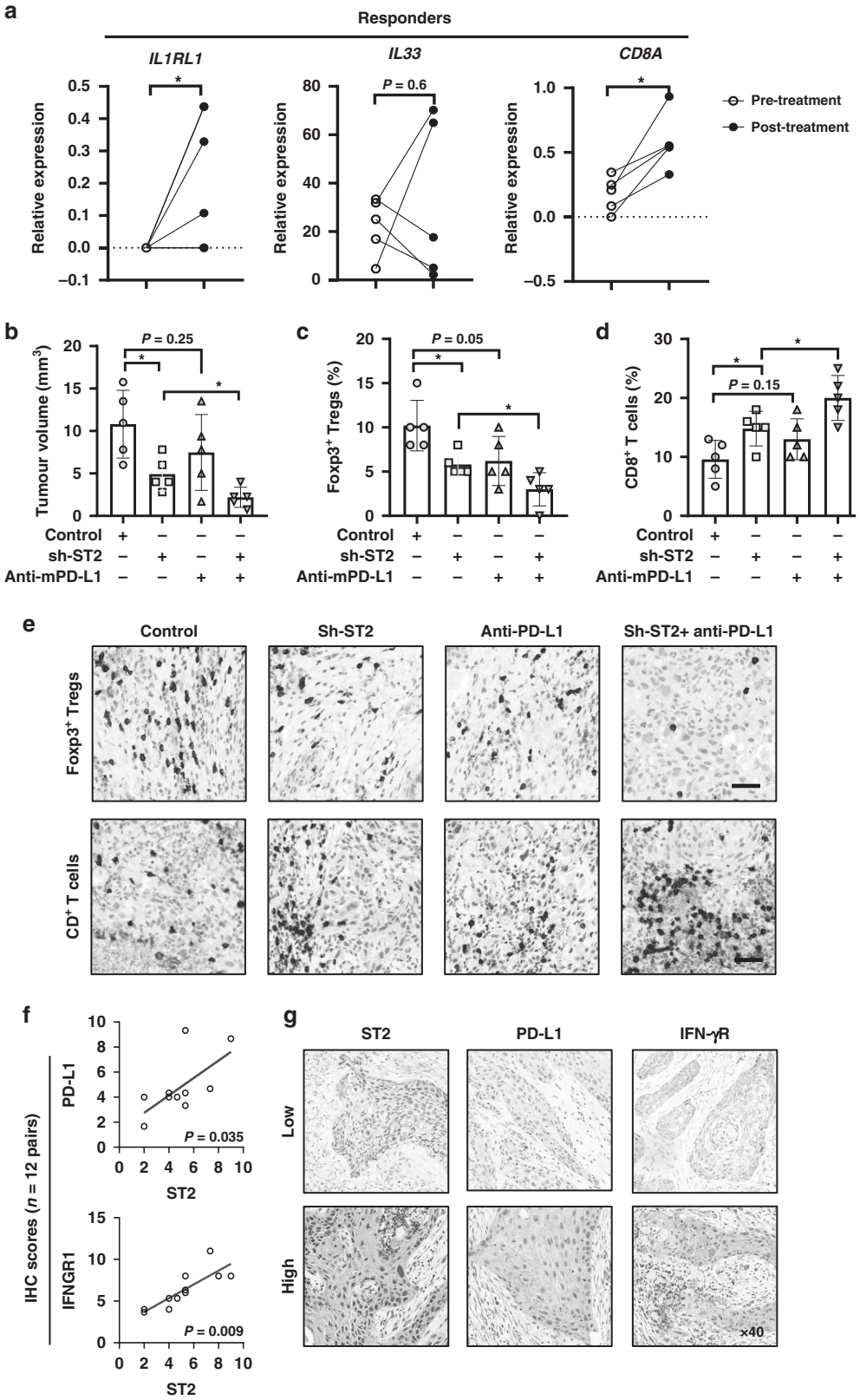

Fig. 6 ST2 knockdown combines with anti-PD-L1 therapy show superior anti-tumor effects in OSCC. a The transcriptomic features of response in pre- or post-treatment responder tumors from anti-PD-1 therapy for resectable oral squamous cell carcinoma were analyzed (GSE179730). **b–e** C57BL/6 mice with no immunodeficiency was used to establish orthotopic xenograft tongue tumor model by control or ST2-knockdown SCC7 cells. Anti-mPD-L1 or IgG isotype control was treated, 200 μg/mice, i.p., every 2 days. Tumor weight were determined, and $CD8^+$ T cells, $Foxp3^+$ Tregs in tumor tissues were analyzed by immunohistochemistry. **f**, **g** IHC result of the expression correlation between ST2 and PD-L1 and IFN-γR in 12 OSCC patients. Results are shown as mean ± SEM. *$p < 0.05$, **$p < 0.01$, ***$p < 0.001$. p = Two-tailed t test.

mice with no immunodeficiency were used. In orthotopic xenograft tongue tumor model (Supplementary Fig. 2a), treatment of recombinant IL-33 or ST2 overexpressed tumor cells induced significant tumor growth in vivo. Tumor tissues showed increased $Foxp3^+$ Tregs infiltration and reduced $CD8^+$ T cells ratio (Supplementary Fig. 2b–d). Additionally, anti-PD-1 therapy alone in control group showed no significant impacts on the proportion of $Foxp3^+$ Tregs, but increased 6.4% $CD8^+$ T cells infiltration, and inhibited tumor growth, although not significantly (Supplementary Fig. 2e). However, anti-PD-L1 therapy in tumors with IL33/ST2 activation significantly induced tumor regression and abrogated ST2/PD-L1-induced immunosuppression. Tumor infiltrated $Foxp3^+$ Tregs were reduced 9% and $CD8^+$ T cells were increased 10.4% (Supplementary Fig. 2f).

We further analyzed the transcriptomic features of response in pre- and post-treatment tumors from anti-PD-1 therapy for resectable oral squamous cell carcinoma [28]. Therapy responders have higher expression of *CD274*, *IL33*, *IL1RL1*, *JAK2* and *TRAF6* than non-responders. TIGIT as an inhibitory receptor expressed by activated T cells was up-regulated in non-responders (Supplementary Fig. 3a–f). Besides, after PD-1 blockade treatment, tumor from responders showed more *CD8* expression and *ST2* level, which provided a basis for testing rational combination treatments of ST2 inhibition and PD-1/L1 blockade (Fig. 6a). Indeed, ST2 knockdown combined with anti-PD-L1 therapy showed superior anti-tumor effects with increased $CD8^+$ T cells and reduced $Foxp3^+$ Tregs as shown in (Fig. 6b–e).

Finally, we verified the ST2/IFN-γR/PD-L1 pathway in situ in OSCC patients ($n = 12$) by IHC staining. The protein expression of ST2, PD-L1 and IFN-γR in OSCC clinical samples were estimated by staining area and intensity. The results showed that the expression location of ST2, PD-L1 and IFN-γR were observed in tumor cells in OSCC, and high ST2 expression significantly correlated with high PD-L1, IFN-γR expression (Fig. 6f, g). Therefore, evidences in vitro, in vivo and clinical data together illustrated a IL-33/ST2/PD-L1-based immune regulation model (Supplementary Fig. 4): When tumor shows low ST2/PD-L1 expression, more activated T cells and IFN-γ present in tumor microenvironment and the tumor progression is inhibited. However, when tumor shows up-regulated ST2 expression, IL-33 and IFN-γ induced more PD-L1 expression and less activated T cells in tumor microenvironment, which leads to tumor progression. But $ST2^+$ tumor patients with high PD-L1 might be more vulnerable to the anti-PD-1/L1 therapy.

DISCUSSION

The stromal cells in the surrounding TME, such as the CAFs, not only act as an active contributor to cancer growth, but CAF-derived factors involved in the upregulation of PD-L1 in different tumor cell types for immune escape [29, 30]. Through the secretion of soluble factors like CXCL2, α-SMA^+CAFs can increase PD-L1 expression in lung adenocarcinoma cells, thereby influencing antitumor immunity [31]. Recent studies have revealed some detailed intracellular signaling mechanisms. As shown in the research by Zhang et al, CAFs in colorectal cancer facilitate extracellular signal regulated kinase 5 (ERK5) expression and phosphorylation to increase the synthesis of PD-L1 protein [32]. On the basis of the fact that CAFs were the important source of IL-33 and participated into immune escape [15, 33], we here found that IL-33 mainly located in OSCC stroma fibroblast, which might create opportunities for stroma IL-33 to activate $ST2^+$ tumor cells to induce PD-L1 expression for immunosuppression.

Previous studies have shown that constitutive PD-L1 expression involves PTEN deletions, EGFR mutations or JAK1/2 mutations; whereas both type I and II interferons (IFN) contribute to the inducible PD-L1 expression, especially interferon-γ (IFN-γ) [34, 35]. IFN-γ is a key driver of PD-L1 expression in host tumors, whereas IL-33 can stimulate a variety of immune cell responses, including IFN-γ production by stimulating activated $CD8^+$T cells, and IL-1β, IL-6, TNF-α from macrophages and mast cells [36–38]. These cytokines are known stimulators of PD-L1. However, most of the existing studies only focus on the functional regulation of IL-33 on immune cells. In this study, we found that stroma IL-33 activated ST2 signaling of tumor cells, leading to the constitutive PD-L1 on OSCC cells via JAK-STAT3. Indeed, activity of JAK was essential for PD-L1 expression in many cancer types [3].

ST2 activation was reported to activate diverse intracellular kinases and factors (e.g. MyD88, IRAK-1, IRAK-4, and TRAF-6) and increase the transcription activity of NF-kB, p-38, JNK, and ERK for downstream inflammatory genes expressions and ultimately to the production of inflammatory cytokines/chemokines and mounting of an adequate immune response [39–41]. Notably, *IFNGR* expression induced by IL-1 were found to be dependent on NF-kB transactivation in epithelial cells [27]. Our research showed that the stimulation of IL-33 could activate NF-kB signaling and promote IFN-γR expression in tumor cells. Thus we speculated that IL-33 increased the expression of IFN-γR in tumor cells, which showed enhanced response to the $CD8+$T cells-derived IFN-γ and PD-L1 expression in tumor microenvironment.

Our data show that stroma IL-33 could activate JAK2/STAT3 phosphorylation of $ST2^+$ tumor cells and promote the expression of PD-L1. IL-33/ST2 can also activates the expression of IFN-γR through MyD88/TRAF6/NF-κB signaling to indirectly stimulates IFN-γ-induced PD-L1 expression. These findings revealed a complex tumor-promoting microenvironment shaped by IL-33/ST2 axis in OSCC. Inhibition of ST2 signaling might benefit for anti-PD-1/L1 therapy of OSCC patients.

DATA AVAILABILITY

All of the data generated or analyzed in this study are included in this published article.

REFERENCES

1. Burtness B, Harrington KJ, Greil R, Soulieres D, Tahara M, de Castro G Jr, et al. Pembrolizumab alone or with chemotherapy versus cetuximab with chemotherapy for recurrent or metastatic squamous cell carcinoma of the head and neck (KEYNOTE-048): a randomised, open-label, phase 3 study. Lancet. 2019;394:1915–28.
2. Cramer JD, Burtness B, Ferris RL. Immunotherapy for head and neck cancer: Recent advances and future directions. Oral Oncol. 2019;99:104460.
3. Ribas A, Hu-Lieskovan S. What does PD-L1 positive or negative mean? J Exp Med. 2016;213:2835–40.
4. Shen X, Zhao B. Efficacy of PD-1 or PD-L1 inhibitors and PD-L1 expression status in cancer: meta-analysis. BMJ. 2018;362:k3529.
5. Pires da Silva I, Ahmed T, Reijers ILM, Weppler AM, Betof Warner A, Patrinely JR, et al. Ipilimumab alone or ipilimumab plus anti-PD-1 therapy in patients with metastatic melanoma resistant to anti-PD-(L)1 monotherapy: a multicentre, retrospective, cohort study. Lancet Oncol. 2021;22:836–47.
6. Yi M, Jiao D, Xu H, Liu Q, Zhao W, Han X, et al. Biomarkers for predicting efficacy of PD-1/PD-L1 inhibitors. Mol Cancer. 2018;17:129.
7. Saigi M, Alburquerque-Bejar JJ, Mc Leer-Florin A, Pereira C, Pros E, Romero OA, et al. MET-oncogenic and JAK2-inactivating alterations are independent factors that affect regulation of PD-L1 expression in lung cancer. Clin Cancer Res. 2018;24:4579–87.
8. Barroso-Sousa R, Keenan TE, Pernas S, Exman P, Jain E, Garrido-Castro AC, et al. Tumor mutational burden and PTEn alterations as molecular correlates of response to PD-1/L1 blockade in metastatic triple-negative breast cancer. Clin Cancer Res. 2020;26:2565–72.
9. Yu M, Peng Z, Qin M, Liu Y, Wang J, Zhang C, et al. Interferon-gamma induces tumor resistance to anti-PD-1 immunotherapy by promoting YAP phase separation. Mol Cell. 2021;81:1216–30.e1219.
10. Wu T, Dai Y. Tumor microenvironment and therapeutic response. Cancer Lett. 2017;387:61–68.
11. Feng J, Yang H, Zhang Y, Wei H, Zhu Z, Zhu B, et al. Tumor cell-derived lactate induces TAZ-dependent upregulation of PD-L1 through GPR81 in human lung cancer cells. Oncogene. 2017;36:5829–39.
12. Gordon SR, Maute RL, Dulken BW, Hutter G, George BM, McCracken MN, et al. PD-1 expression by tumour-associated macrophages inhibits phagocytosis and tumour immunity. Nature. 2017;545:495–9.

13. Noman MZ, Desantis G, Janji B, Hasmim M, Karray S, Dessen P, et al. PD-L1 is a novel direct target of HIF-1alpha, and its blockade under hypoxia enhanced MDSC-mediated T cell activation. J Exp Med. 2014;211:781–90.
14. Feig C, Jones JO, Kraman M, Wells RJ, Deonarine A, Chan DS, et al. Targeting CXCL12 from FAP-expressing carcinoma-associated fibroblasts synergizes with anti-PD-L1 immunotherapy in pancreatic cancer. Proc Natl Acad Sci USA. 2013;110:20212–7.
15. Ding L, Ren J, Zhang D, Li Y, Huang X, Hu Q, et al. A novel stromal lncRNA signature reprograms fibroblasts to promote the growth of oral squamous cell carcinoma via LncRNA-CAF/interleukin-33. Carcinogenesis. 2018;39:397–406.
16. Zhao X, Ding L, Lu Z, Huang X, Jing Y, Yang Y, et al. Diminished CD68(+) cancer-associated fibroblast subset induces regulatory T-cell (Treg) infiltration and predicts poor prognosis of oral squamous cell carcinoma patients. Am J Pathol. 2020;190:886–99.
17. Wang Y, Jing Y, Ding L, Zhang X, Song Y, Chen S, et al. Epiregulin reprograms cancer-associated fibroblasts and facilitates oral squamous cell carcinoma invasion via JAK2-STAT3 pathway. J Exp Clin cancer Res: CR. 2019;38:274.
18. Ding L, Ren J, Zhang D, Li Y, Huang X, Ji J, et al. The TLR3 agonist inhibit drug efflux and sequentially consolidates low-dose cisplatin-based chemoimmunotherapy while reducing side effects. Mol Cancer Ther. 2017;16:1068–79.
19. Cayrol C, Girard JP. Interleukin-33 (IL-33): A nuclear cytokine from the IL-1 family. Immunol Rev. 2018;281:154–68.
20. Son J, Cho JW, Park HJ, Moon J, Park S, Lee H, et al. Tumor-infiltrating regulatory T-cell accumulation in the tumor microenvironment is mediated by IL33/ST2 signaling. Cancer Immunol Res. 2020;8:1393–406.
21. Wen YH, Lin HQ, Li H, Zhao Y, Lui VWY, Chen L, et al. Stromal interleukin-33 promotes regulatory T cell-mediated immunosuppression in head and neck squamous cell carcinoma and correlates with poor prognosis. Cancer Immunol Immunother. 2019;68:221–32.
22. Ding Z, He Y, Fu Y, Zhu N, Zhao M, Song Y, et al. CD38 multi-functionality in oral squamous cell carcinoma: prognostic implications, immune balance, and immune checkpoint. Front Oncol. 2021;11:687430.
23. Ayers M, Lunceford J, Nebozhyn M, Murphy E, Loboda A, Kaufman DR, et al. IFN-gamma-related mRNA profile predicts clinical response to PD-1 blockade. J Clin Invest. 2017;127:2930–40.
24. Griesenauer B, Jiang H, Yang J, Zhang J, Ramadan AM, Egbosiuba J, et al. ST2/MyD88 deficiency protects mice against acute graft-versus-host disease and spares regulatory T cells. J Immunol. 2019;202:3053–64.
25. Griesenauer B, Paczesny S. The ST2/IL-33 axis in immune cells during inflammatory diseases. Front Immunol. 2017;8:475.
26. Wang L, Luo Y, Luo L, Wu D, Ding X, Zheng H, et al. Adiponectin restrains ILC2 activation by AMPK-mediated feedback inhibition of IL-33 signaling. J Exp Med. 2021;218:e20191054.
27. Shirey KA, Jung JY, Maeder GS, Carlin JM. Upregulation of IFN-gamma receptor expression by proinflammatory cytokines influences IDO activation in epithelial cells. J Interferon Cytokine Res. 2006;26:53–62.
28. Liu S, Knochelmann HM, Lomeli SH, Hong A, Richardson M, Yang Z, et al. Response and recurrence correlates in individuals treated with neoadjuvant anti-PD-1 therapy for resectable oral cavity squamous cell carcinoma. Cell Rep. Med. 2021;2:100411.
29. Dominguez CX, Muller S, Keerthivasan S, Koeppen H, Hung J, Gierke S, et al. Single-cell RNA sequencing reveals stromal evolution into LRRC15(+) myofibroblasts as a determinant of patient response to cancer immunotherapy. Cancer Disco. 2020;10:232–53.
30. Galbo PM Jr, Zang X, Zheng D. Molecular features of cancer-associated fibroblast subtypes and their implication on cancer pathogenesis, prognosis, and immunotherapy resistance. Clin Cancer Res. 2021;27:2636–47.
31. Inoue C, Miki Y, Saito R, Hata S, Abe J, Sato I, et al. PD-L1 induction by cancer-associated fibroblast-derived factors in lung adenocarcinoma cells. Cancers (Basel). 2019;11:1257.
32. Zhang M, Shi R, Guo Z, He J. Cancer-associated fibroblasts promote cell growth by activating ERK5/PD-L1 signaling axis in colorectal cancer. Pathol Res Pract. 2020;216:152884.
33. Lin Y, Cai Q, Chen Y, Shi T, Liu W, Mao L, et al. CAFs shape myeloid-derived suppressor cells to promote stemness of intrahepatic cholangiocarcinoma through 5-lipoxygenase. Hepatology. 2022;75:28–42.
34. Peng S, Wang R, Zhang X, Ma Y, Zhong L, Li K, et al. EGFR-TKI resistance promotes immune escape in lung cancer via increased PD-L1 expression. Mol Cancer. 2019;18:165.
35. Guo Y, Song J, Wang Y, Huang L, Sun L, Zhao J, et al. Concurrent genetic alterations and other biomarkers predict treatment efficacy of EGFR-TKIs in EGFR-mutant non-small cell lung cancer: a review. Front Oncol. 2020;10:610923.
36. Clark JT, Christian DA, Gullicksrud JA, Perry JA, Park J, Jacquet M, et al. IL-33 promotes innate lymphoid cell-dependent IFN-gamma production required for innate immunity to Toxoplasma gondii. Elife 2021;10:e65614.
37. Hatzioannou A, Banos A, Sakelaropoulos T, Fedonidis C, Vidali MS, Kohne M, et al. An intrinsic role of IL-33 in Treg cell-mediated tumor immunoevasion. Nat Immunol. 2020;21:75–85.
38. Park SH, Kim MS, Lim HX, Cho D, Kim TS. IL-33-matured dendritic cells promote Th17 cell responses via IL-1beta and IL-6. Cytokine. 2017;99:106–13.
39. Ganesan S, Pham D, Jing Y, Farazuddin M, Hudy MH, Unger B, et al. TLR2 activation limits rhinovirus-stimulated CXCL-10 by attenuating IRAK-1-dependent IL-33 receptor signaling in human Bronchial epithelial cells. J Immunol. 2016;197:2409–20.
40. Schmitz J, Owyang A, Oldham E, Song Y, Murphy E, McClanahan TK, et al. IL-33, an interleukin-1-like cytokine that signals via the IL-1 receptor-related protein ST2 and induces T helper type 2-associated cytokines. Immunity. 2005;23:479–90.
41. Choi YS, Choi HJ, Min JK, Pyun BJ, Maeng YS, Park H, et al. Interleukin-33 induces angiogenesis and vascular permeability through ST2/TRAF6-mediated endothelial nitric oxide production. Blood. 2009;114:3117–26.

AUTHOR CONTRIBUTIONS

Conceptualization: LD, YHN and ZYW; data curation: MXZ; formal analysis: MXZ and YXS; methodology: LD, NSZ and YJH, and MXZ; investigation: NSZ, and MXZ; supervision: LD, YHN, and QGH; validation: YHN; Writing—original draft: LD and MXZ.

FUNDING

Research was supported by grants by the National Natural Science Foundation of China (Grant No. 81902754, 82002865); Natural Science Foundation of Jiangsu Province (No. BK20190304, BE2020628); Nanjing Medical Science and Technology Development Foundation, Nanjing Department of Health (No. YKK21182, YKK20151).

COMPETING INTERESTS

The authors declare no competing interests.

ETHICS APPROVAL AND CONSENT TO PARTICIPATE

Ethical approval for this study including tumor biopsy and serum collection was obtained from the Research Ethics Committee of Nanjing Stomatology Hospital (No.2019NL-009(KS)) and informed consent was obtained from the patients. The study was performed in accordance with the Declaration of Helsinki. All animal experiments were performed in accordance with Jiangsu Association for Laboratory Animal Science (Authorization Number: 220195073) and were subject to review by the animal welfare and ethical review board of Nanjing university.

ADDITIONAL INFORMATION

Supplementary information The online version contains supplementary material available at https://doi.org/10.1038/s41416-022-02090-0.

Correspondence and requests for materials should be addressed to Zhiyong Wang, Yanhong Ni or Liang Ding.